



**HAL**  
open science

## Impact of the multilayer dielectric design on the laser-induced damage threshold of pulse compression gratings for petawatt-class lasers

Saaxewer Diop, Nicolas Bonod, Marine Chorel, Éric Lavastre, Nadja Roquin, Lilian Heymans, Pierre Brianceau, Laurent Gallais, Laurent Lamaignère

### ► To cite this version:

Saaxewer Diop, Nicolas Bonod, Marine Chorel, Éric Lavastre, Nadja Roquin, et al.. Impact of the multilayer dielectric design on the laser-induced damage threshold of pulse compression gratings for petawatt-class lasers. *Optics Letters*, 2023, 48 (17), pp.4669. 10.1364/OL.498295 . hal-04308683

**HAL Id: hal-04308683**

**<https://cnrs.hal.science/hal-04308683>**

Submitted on 27 Nov 2023

**HAL** is a multi-disciplinary open access archive for the deposit and dissemination of scientific research documents, whether they are published or not. The documents may come from teaching and research institutions in France or abroad, or from public or private research centers.

L'archive ouverte pluridisciplinaire **HAL**, est destinée au dépôt et à la diffusion de documents scientifiques de niveau recherche, publiés ou non, émanant des établissements d'enseignement et de recherche français ou étrangers, des laboratoires publics ou privés.

# Impact of the multilayer dielectric design on the laser-induced damage threshold of pulse compression gratings for petawatt-class lasers

SAAXEWER DIOP<sup>1,2,\*</sup>, NICOLAS BONOD<sup>2</sup>, MARINE CHOREL<sup>1</sup>, ÉRIC LAVASTRE<sup>1</sup>, NADJA ROQUIN<sup>1</sup>, LILIAN HEYMANS<sup>1</sup>, PIERRE BRIANCEAU<sup>3</sup>, LAURENT GALLAIS<sup>2</sup>, AND LAURENT LAMAIGNÈRE<sup>1</sup>

<sup>1</sup>CEA-CESTA, F-33116 Le Barp, France

<sup>2</sup>Aix-Marseille Univ, CNRS, Centrale Marseille, Institut Fresnel, 13013 Marseille, France

<sup>3</sup>CEA-GRENOBLE, F-38054 Grenoble, France

\*Corresponding author: diop1@llnl.gov

Compiled July 18, 2023

The peak-power of petawatt-class lasers is limited by laser-induced damage to final optical components, especially on the pulse compression gratings. Multilayer Dielectric (MLD) gratings are widely used in compressor systems because they exhibit a high diffraction efficiency and high damage threshold. It is now well established that the etching profile plays a key role in the electric field distribution, which influences the laser damage resistance of MLD gratings. However, less attention has been devoted to the influence of the multilayer design on the laser damage resistance of MLD gratings. In this paper, we numerically and experimentally evidence the impact of the dielectric stack design on the Electric Field Intensity (EFI) and the laser-induced damage threshold (LIDT). Three different MLD gratings are designed and manufactured to perform laser damage tests. On the basis of the expected EFIs and diffraction efficiencies, the measured LIDTs show how the multilayer design influences the laser resistance of the MLD gratings. This result highlights the impact of the multilayer dielectric design on the electric field distribution and shows how to further improve the laser-induced damage threshold of pulse compression gratings. © 2023 Optica Publishing Group

<http://dx.doi.org/10.1364/ao.XX.XXXXXX>

Ultra-fast laser facilities have reached a new level of power since the development of the Chirped Pulse Amplification (CPA) technique [1]. The peak power remains limited by laser-induced damage to components in and after the compressor system, which explains why pulse compression gratings are critical components of petawatt laser facilities. Multilayer Dielectric (MLD) pulse compression gratings are of particular interest due to their high laser induced damage threshold and high diffraction efficiency. Svakhin *et al.* demonstrated first the feasibility of diffraction gratings made with dielectric materials [2]. A few months later, Perry *et al.* evidenced the improvement of

the Laser-Induced Damage Threshold (LIDT) of MLD gratings compared to metallic gratings for similar ranges of diffraction efficiencies [3].

A lot of studies have been carried out to improve the LIDT of MLD gratings by optimizing the design, the manufacturing, and the cleaning processes [4–7]. MLD gratings are generally designed in two steps: the MLD stack is defined to maximize the reflectivity at the conditions of operation, such as angle of incidence, polarization, and wavelength. Then, the etching profile is added on the top layer and the parameters are defined to maximize the diffraction efficiency. The grating profile has a strong influence on the EFI. In particular, for a given period and condition of illumination, small duty cycles must be privileged since they allow to strongly decrease the EFI inside the pillars [8]. The strong influence of the etching profile on the EFI and therefore on the laser induced damage threshold of MLD gratings was evidenced experimentally in Ref. [9].

In this paper, we investigate the influence of the dielectric stack on the electric field distribution to optimize the laser resistance of pulse compression gratings of the PETAL facility [10]. The optimization relies on the reduction of the electric field intensity (EFI). Chorel *et al.* demonstrated an important improvement in the LIDT of the PETAL dielectric mirrors by modifying the layer thicknesses [11]. Based on these results, we develop a method to optimize MLD gratings. Starting with a given MLD stack, we defined the etching profile to maximize the diffraction efficiency. Then, we reduced the EFI by modifying the thickness of several upper layers. The electric field distribution and the diffraction efficiency were calculated numerically, and 3 designs were manufactured to perform laser damage tests to assess the numerical results.

Pulse compression gratings of PETAL laser operate in reflection, in *s*-polarization with an angle of incidence of 77.2° at a wavelength of 1053 nm. To calculate the performances of a grating design, we used a numerical model developed to calculate the diffraction efficiency and the electric field distribution. The model is based on the differential method with the fast Fourier factorization and the S-algorithm to solve the Maxwell's equations [12–15]. The model allows different input parameters to

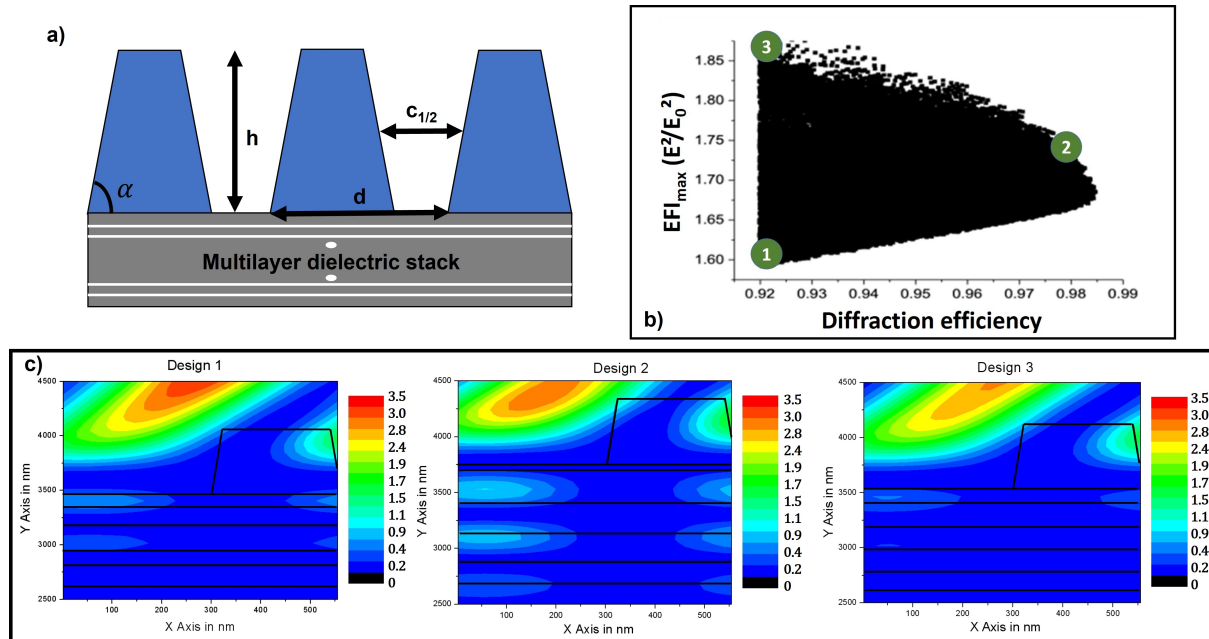


**Fig. 1.** (a) Representation of an etching profile in the top layer of the MLD stack. The profile is etched with a grating period  $d$ . The pillars have a trapezoidal shape with depth  $h$  and a slope angle  $\alpha$ . The thickness  $DC$  at mid-height of the pillars corresponds to the Duty Cycle ( $DC = 1 - \frac{c_1}{2}$ ). (b) Representation of the performances in terms of EFI and diffraction efficiency of the 14000 designs selected from the computational model. Only designs with a diffraction efficiency greater than 92% were selected. Each design is represented by a square plotted in terms of the EFI and diffraction efficiency associated with the design. The green dots represent the 3 designs selected for the fabrication of the samples. See [Data file 1](#) for the description of the entire design. (c) Representation of the electric field distribution in the pillars and the top layers of the selected designs 1, 2, 3, represented in (b): design 1 represents the design with the lowest EFI value; design 3 represents the design with the highest EFI value and a similar diffraction efficiency to design 1; design 2 represents the third point of comparison and a trade-off between EFI and diffraction efficiency (see [Tab. 1](#)). Calculations are performed by considering a plane wave illuminating the grating from the top (superstrate) with an angle of incidence of  $+77.2^\circ$ .

be incremented over a defined range and step, such as etching parameters or layer thicknesses. The model explores all possible combinations using the brute force method and calculates the grating performances of each design.

We paid special attention to the supply of samples when designing the gratings. The manufacturing capabilities and constraints of the suppliers have been taken into account. To limit deviations, we considered a single etching profile.

First, we started with a given MLD stack used for previous PETAL gratings. The design was [Borofloat / (LH)<sup>10</sup> L / Air] where L and H represent the SiO<sub>2</sub> and HfO<sub>2</sub> layers respectively. **The refractive indexes of HfO<sub>2</sub> and SiO<sub>2</sub> materials are taken equal to 1.430 and 1.826, respectively.** The etching profile was defined in the top layer with trapezoidal shape (see [Fig. 1\(a\)](#)). The duty cycle and the slope angle were set to values with the lowest probability of deviation due to the fabrication process at 0.44 and 88° respectively. The period is fixed by the PETAL compressor specification at 562 nm. We do not consider a residual thickness under the pillars, which is a source of potential deviations. We maximized the diffraction efficiency by exploring different values of the etching depth over a range between 400 nm and 800 nm, with a step of 10 nm. The results show that a depth of 590 nm leads to a diffraction efficiency greater than 98%. Next, we modified the MLD stack to reduce the EFI. We perform a parametric optimization as a function of the 7 upper layers. The variation range of each layer is equal to 100 nm, with an incremental step of 10 nm. The model explored 10<sup>7</sup>

combinations. Designs with a diffraction efficiency greater than 92% were selected.

[Figure 1\(b\)](#) represents the distribution of the 14000 solutions selected that exhibit a diffraction efficiency in the -1st order higher than 92%. They are represented as a function of the EFI and diffraction efficiency. In the narrow 92%-93% efficiency range, we observed that gratings show discrepancies of EFI values up to 13%. It clearly shows the impact of the MLD stack on the EFI values. We selected three designs to manufacture samples (see [Fig. 1\(b\)](#)): design 1 represents the design with the lowest EFI value; design 3 represents the design with the highest EFI value and a similar diffraction efficiency to design 1; design 2 represents the third point of comparison and a trade-off between EFI and diffraction efficiency (see [Tab. 1](#)). [Figure 1\(c\)](#) shows the electric field distribution and the variation of the layer thicknesses between each design (see [Data file 1](#)). The highest EFI value is localized for the three designs in the upper right side of the pillars for an incident beam coming from the left at an incidence of 77.2°.

The process of the manufacturing of the three samples is detailed in [Fig. 2\(a\)](#). First, the MLD stack was deposited through an e-beam evaporation process on borofloat substrate. The supplier responsible for the etching process used UV optical lithography, which is usually used for etching semiconductors. Therefore, a second step was implemented to make the samples compatible with the micro-electronics machines. These instruments work with detectors in the visible range. However, the substrate and

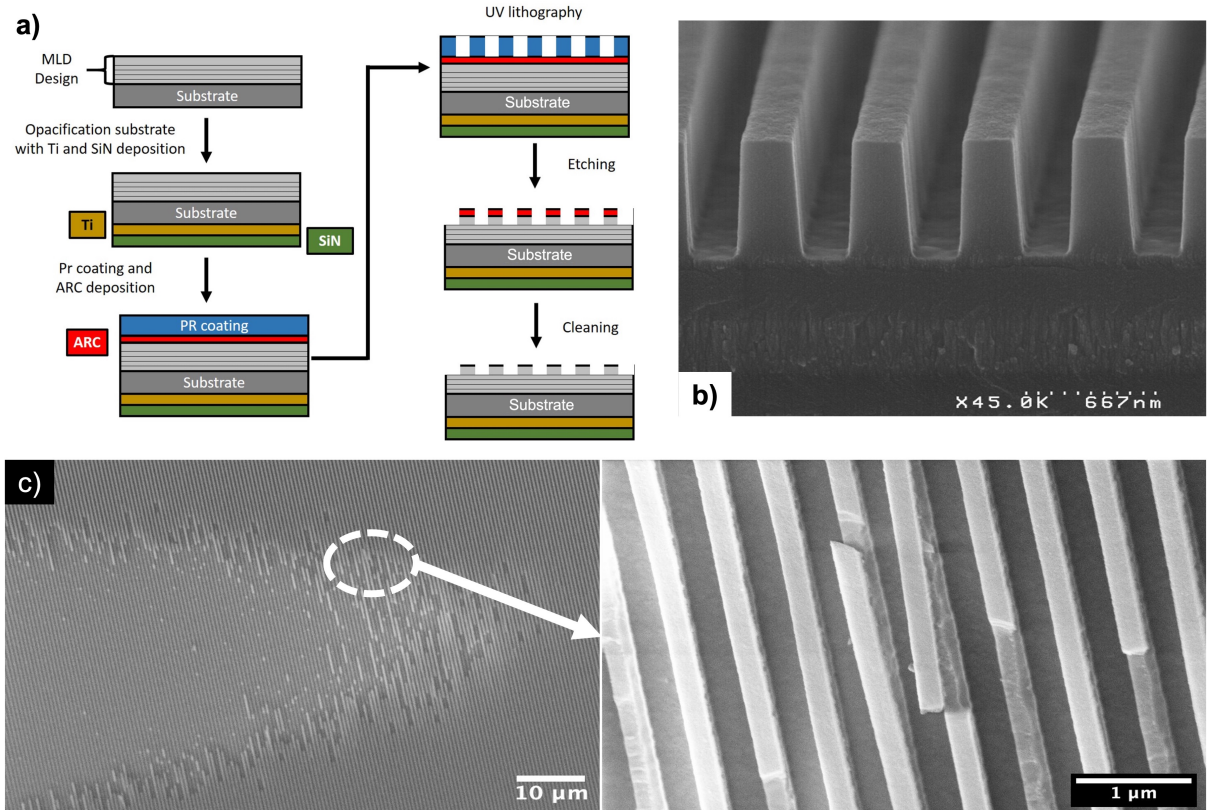


**Fig. 2.** (a) Representation of the grating sample process flow. First, the MLD stack is deposited on the borofloat substrate. Then, SiN and Ti layers are deposited on the backside of the substrate to opacify the samples. An anti-reflective and a photosensitive resin coatings are deposited on the MLD stack. Optical lithography records the pattern in the resin, which is then etched to obtain the final structure. SEM observations of (b) the manufactured etching profile **which is representative of all designs** and (c) a laser damage site of 1-on-1 tests. The image of the right corresponds to a zoom of the dashed zone.

**Table 1.** Numerical features of the 3 selected designs.

Designs	EFI <sub>max</sub>	DE (-1R)
1	1.63	92.8%
2	1.75	98.2%
3	1.88	92.4%

the dielectric stack are transparent in this wavelength range. A layer of Ti was deposited on the back side of the substrate to opacify the substrate and thus make it detectable by the instruments. A layer of SiN was also deposited to ensure the lift-off of the plates from the sample holder after electrostatic clamping. Then, an anti-reflective coating (ARC) and a layer of photosensitive resin coating (PRC) were deposited on the dielectric stack. The ARC layer aims to reduce reflections at the recording wavelength of the etching pattern, i.e., 248 nm. A mask placed on the optical path of the laser allows to print the etching profile in the PRC. Dry etching was performed to etch the top SiO<sub>2</sub> layer. A plasma composed of N<sub>2</sub>O<sub>2</sub> and C<sub>4</sub>F<sub>8</sub> reacted with the solid SiO<sub>2</sub>. The etching depth depends on the reaction time and during tests, the HfO<sub>2</sub> layer underneath the etching was difficult to identify compared to the SiO<sub>2</sub> layer. To remedy this issue, we have chosen to keep a residual thickness of 30 nm under the pillars. Finally, a cleaning process allows removing all the

125 reaction residues, especially the PRC and the ARC. Figure 2(b)  
 126 shows an SEM observation of the final etching. **The DC featured**  
 127 **by the manufactured grating, estimated at roughly 0.50, slightly**  
 128 **differs from the DC used to perform the numerical designs and**  
 129 **simulations (DC=0.44).** With this new etching profile, we calculated the new performances of each design. We considered possible deviation of the etching parameters over a range of 30 nm (4° for the slope angle) and a step of 5 nm (1°). The results are presented in Tab. 2 with average values. The uncertainties corresponding to the standard deviation.

135 Laser damage tests were performed on the dedicated optical  
 136 set-up called DERIC at the French Atomic Commission (CEA-  
 137 CESTA), described in Ref. [16]. A commercial Amplitude laser  
 138 source provides a beam centered at 1053 nm with a pulse duration  
 139 of 800 fs. The output energy is around 2 mJ with a repetition  
 140 rate of 10 Hz. A 60 cm focal lens focuses the beam to obtain at  
 141 the focal plan a Gaussian beam of diameter 160 μm at 1/e. We  
 142 performed 1-on-1 damage tests on each sample to determine  
 143 the laser induced damage threshold (LIDT) [17]. Tests were carried  
 144 out at 77.2° of incidence (operating incident angle of the  
 145 gratings), 5 shots per fluence were set.

146 Results are shown in Tab. 2. We evidence that design 1 with  
 147 the lowest EFI<sub>max</sub> value corresponds to the design with the  
 148 highest LIDT and inversely, design 3 with the highest EFI<sub>max</sub>  
 149 value corresponds to the design with the lowest LIDT. Let us  
 150 point out the differences in LIDT are equivalent to the differences  
 151 in EFI between each design.

**Table 2.** 1-on-1 tests results and calculated features of manufactured designs.

Designs	EFI <sub>max</sub>	$\frac{EFI_1}{EFI_1}$	LIDT (J/cm <sup>2</sup> )	$\frac{LIDT_1}{LIDT_1}$	LIDT <sub>int</sub> (J/cm <sup>2</sup> )
1	1.70 ± 0.13	/	3.67 ± 0.01	/	6.23
2	1.78 ± 0.09	+5%	3.49 ± 0.09	-5%	6.21
3	1.91 ± 0.08	+12%	3.19 ± 0.01	-13%	6.09

Taking design 1 as a reference value, an increase of approximately 5% and 12% in EFI was calculated for designs 2 and 3 respectively. Regarding the laser resistance, a decrease of 5% and 13%, for designs 2 and 3 was measured compared to design 1 respectively. The experimental results are therefore coherent with the theoretical results. In addition, the calculation of the theoretical intrinsic damage threshold ( $LIDT_{int} = EFI_{max} \times LIDT$ ) reveals very close results between designs 1 and 2, but a deviation with design 3. This deviation may be the consequence of manufacturing errors inducing a variation of the  $EFI_{max}$ . The intrinsic LIDTs are very close and highlight a final etching profile close to the profile defined in numerical simulations. By fixing the etching profile, we demonstrated an improvement of the LIDT by an optimization of the MLD design. Scanning electron microscopy (SEM) observations of the damage sites evidence that a portion of the pillars are ablated during the irradiation (see Fig. 2(c)) while the MLD stack seems to be unaffected. This result is concordant with the numerical simulations that predict a maximum of the EFI (see Fig. 1(c)) on the nanostructured pillars [18].

To conclude, we investigated the influence of the MLD stack on the electric field distribution of compression gratings. The objective was to reduce the EFI by adjusting the thicknesses of the upper layers. First, we started with a given MLD stack design, and we defined the etching profile which maximizes the diffraction efficiency. In a second step, we performed a parametrical optimization of the EFI as a function of the thicknesses of the 7 top layers of the multilayer, for a specific and constant etching profile. We selected designs with diffraction efficiencies greater than 92%. We obtained designs with similar diffraction efficiencies, but with discrepancies in terms of EFI up to 13%. We manufactured three samples to perform laser damage tests. The experimental results follow the numerical predictions of the EFI, we found equivalent deviation of laser damage threshold than EFI values. These results demonstrate clearly the impact of the MLD stack on the electric field distribution of a grating and consequently the laser damage threshold.

Manufacturing constraints limit the optimization of the etching profile, which is the most sensitive part of grating manufacturing. Production errors of the etching can impact the performance of the grating. With this approach, it is possible to define a supplier-optimized etching profile and then optimize the LIDT of the grating through the MLD design. The next step of this work will be to find a protocol to optimize the MLD stack and the etching profile in the same time.

**Acknowledgments.** We would like to thank the Optical Manufacturing Shop group lead by Amy Rigatti of the Laboratory for Laser Energetics for supplying the coating samples and for their interest in developing these dielectric stacks.

**Disclosures.** The authors declare no conflicts of interest.

**Data availability.** Data underlying the results presented in this paper are not publicly available at this time but may be obtained from

the authors upon reasonable request.

## REFERENCES

- D. Strickland and G. Mourou, *Opt. Commun.* **55**, 447 (1985).
- A. S. Svakhin, V. A. Sychugov, and A. E. Tikhomirov, *Quantum Electron.* **24**, 233 (1994).
- M. D. Perry, R. D. Boyd, J. A. Britten, D. Decker, B. W. Shore, C. Shannon, and E. Shults, *Opt. Lett.* **20**, 940 (1995).
- L. Xie, J. Zhang, Z. Zhang, B. Ma, T. Li, Z. Wang, and X. Cheng, *Opt. Express* **29**, 2669 (2021).
- H. T. Nguyen, C. C. Larson, and J. A. Britten, "Improvement of laser damage resistance and diffraction efficiency of multilayer dielectric diffraction gratings by hf etchback linewidth tailoring," in *Laser-Induced Damage in Optical Materials: 2010*, vol. 7842 G. J. Exarhos, V. E. Gruzdev, J. A. Menapace, D. Ristau, and M. J. Soileau, eds., International Society for Optics and Photonics (SPIE, 2010), pp. 416 – 425.
- B. Ashe, C. Giacomini, G. Myhre, and A. W. Schmid, "Optimizing a cleaning process for multilayer dielectric (mld) diffraction gratings," in *Laser-Induced Damage in Optical Materials: 2007*, vol. 6720 G. J. Exarhos, A. H. Guenther, K. L. Lewis, D. Ristau, M. J. Soileau, and C. J. Stolz, eds., International Society for Optics and Photonics (SPIE, 2007), pp. 225 – 232.
- J. A. Britten, W. A. Molander, A. M. Komashko, and C. P. Barty, "Multilayer dielectric gratings for petawatt-class laser systems," in *Laser-Induced Damage in Optical Materials: 2003*, vol. 5273 G. J. Exarhos, A. H. Guenther, N. Kaiser, K. L. Lewis, M. J. Soileau, and C. J. Stolz, eds., International Society for Optics and Photonics (SPIE, 2004), pp. 1 – 7.
- N. Bonod and J. Néauport, *Opt. Commun.* **260**, 649 (2006).
- J. Neauport, E. Lavastre, G. Razé, G. Dupuy, N. Bonod, M. Balas, G. de Villele, J. Flamand, S. Kaladgew, and F. Desserouer, *Opt. Express* **15**, 12508 (2007).
- N. Blanchot, G. Béhar, J. Chapuis, C. Chappuis, S. Chardavoine, J.F.ChARRIER, H.Coïc, C. Damiens-Dupont, J. Duthu, P. Garcia, J. P. Goossens, F. Granet, C. Grosset-Grange, P. Guerin, B. Hebrard, L. Hilsz, L. LAMAINÈRE, T. Lacombe, E. Lavastre, T. Longhi, J. Luce, F. Macias, M. Mangeant, E. Mazataud, B. Minou, T. Morgaint, S. Noailles, J. Neauport, P. Patelli, E. Perrot-Minnot, C. Present, B. Remy, C. Rouyer, N. Santacreu, M. Sozet, D. Valla, and F. Lanièsse, *Opt. Express* **25**, 16957 (2017).
- M. Chorel, T. Lanternier, Éric Lavastre, N. Bonod, B. Bousquet, and J. Néauport, *Opt. Express* **26**, 11764 (2018).
- M. Nevière and E. Popov, *Light Propagation in Periodic Media: Differential Theory and Design* (CRC Press, 2003).
- E. Popov, M. Nevière, and N. Bonod, *J. Opt. Soc. Am. A* **21**, 46 (2004).
- L. Li, *J. Opt. Soc. Am. A* **20**, 655 (2003).
- N. Bonod and J. Neauport, *Adv. Opt. Photon.* **8**, 156 (2016).
- S. Diop, M. Chorel, Éric Lavastre, N. Roquin, L. Gallais, N. Bonod, and L. LAMAINÈRE, *Appl. Opt.* **62**, B126 (2023).
- ISO Standard Nos 21254-1–21254-4* (2011).
- S. Hocquet, J. Neauport, and N. Bonod, *Appl. Phys. Lett.* **99**, 061101 (2011).

## FULL REFERENCES

- 256  
257  
258  
259  
260  
261  
262  
263  
264  
265  
266  
267  
268  
269  
270  
271  
272  
273  
274  
275  
276  
277  
278  
279  
280  
281  
282  
283  
284  
285  
286  
287  
288  
289  
290  
291  
292  
293  
294  
295  
296  
297  
298  
299  
300  
301  
302  
303  
304  
305  
306  
307  
308  
309  
310  
311  
312  
313  
314  
315  
316  
317  
318  
319  
320  
321  
322  
323
- 324  
325  
326
1. D. Strickland and G. Mourou, "Compression of amplified chirped optical pulses," *Opt. Commun.* **55**, 447–449 (1985).
  2. A. S. Svakhin, V. A. Sychugov, and A. E. Tikhomirov, "Diffraction gratings with high optical strength for laser resonators," *Quantum Electron.* **24**, 233 (1994).
  3. M. D. Perry, R. D. Boyd, J. A. Britten, D. Decker, B. W. Shore, C. Shannon, and E. Shults, "High-efficiency multilayer dielectric diffraction gratings," *Opt. Lett.* **20**, 940–942 (1995).
  4. L. Xie, J. Zhang, Z. Zhang, B. Ma, T. Li, Z. Wang, and X. Cheng, "Rectangular multilayer dielectric gratings with broadband high diffraction efficiency and enhanced laser damage resistance," *Opt. Express* **29**, 2669–2678 (2021).
  5. H. T. Nguyen, C. C. Larson, and J. A. Britten, "Improvement of laser damage resistance and diffraction efficiency of multilayer dielectric diffraction gratings by hf etchback linewidth tailoring," in *Laser-Induced Damage in Optical Materials: 2010*, vol. 7842 G. J. Exarhos, V. E. Gruzdev, J. A. Menapace, D. Ristau, and M. J. Soileau, eds., International Society for Optics and Photonics (SPIE, 2010), pp. 416–425.
  6. B. Ashe, C. Giacomini, G. Myhre, and A. W. Schmid, "Optimizing a cleaning process for multilayer dielectric (mld) diffraction gratings," in *Laser-Induced Damage in Optical Materials: 2007*, vol. 6720 G. J. Exarhos, A. H. Guenther, K. L. Lewis, D. Ristau, M. J. Soileau, and C. J. Stolz, eds., International Society for Optics and Photonics (SPIE, 2007), pp. 225–232.
  7. J. A. Britten, W. A. Molander, A. M. Komashko, and C. P. Barty, "Multilayer dielectric gratings for petawatt-class laser systems," in *Laser-Induced Damage in Optical Materials: 2003*, vol. 5273 G. J. Exarhos, A. H. Guenther, N. Kaiser, K. L. Lewis, M. J. Soileau, and C. J. Stolz, eds., International Society for Optics and Photonics (SPIE, 2004), pp. 1–7.
  8. N. Bonod and J. Néauport, "Optical performance and laser induced damage threshold improvement of diffraction gratings used as compressors in ultra high intensity lasers," *Opt. Commun.* **260**, 649–655 (2006).
  9. J. Neauport, E. Lavastre, G. Razé, G. Dupuy, N. Bonod, M. Balas, G. de Villele, J. Flamand, S. Kaladgew, and F. Desserouer, "Effect of electric field on laser induced damage threshold of multilayer dielectric gratings," *Opt. Express* **15**, 12508–12522 (2007).
  10. N. Blanchot, G. Béhar, J. Chapuis, C. Chappuis, S. Chardavoine, J.F. Charrier, H. Coïc, C. Damiens-Dupont, J. Duthu, P. Garcia, J. P. Goossens, F. Granet, C. Grosset-Grange, P. Guerin, B. Hebrard, L. Hilsz, L. Lamoignon, T. Lacombe, E. Lavastre, T. Longhi, J. Luce, F. Macias, M. Mangeant, E. Mazataud, B. Minou, T. Morgaint, S. Noailles, J. Neauport, P. Patelli, E. Perrot-Minnot, C. Present, B. Remy, C. Rouyer, N. Santacreu, M. Sozet, D. Valla, and F. Lanièsse, "1.15 pw-850 j compressed beam demonstration using the petal facility," *Opt. Express* **25**, 16957–16970 (2017).
  11. M. Choulet, T. Lanternier, Éric Lavastre, N. Bonod, B. Bousquet, and J. Néauport, "Robust optimization of the laser induced damage threshold of dielectric mirrors for high power lasers," *Opt. Express* **26**, 11764–11774 (2018).
  12. M. Nevrière and E. Popov, *Light Propagation in Periodic Media: Differential Theory and Design* (CRC Press, 2003).
  13. E. Popov, M. Nevrière, and N. Bonod, "Factorization of products of discontinuous functions applied to fourier-bessel basis," *J. Opt. Soc. Am. A* **21**, 46–52 (2004).
  14. L. Li, "Note on the s-matrix propagation algorithm," *J. Opt. Soc. Am. A* **20**, 655–660 (2003).
  15. N. Bonod and J. Neauport, "Diffraction gratings: from principles to applications in high-intensity lasers," *Adv. Opt. Photon.* **8**, 156–199 (2016).
  16. S. Diop, M. Choulet, Éric Lavastre, N. Roquin, L. Gallais, N. Bonod, and L. Lamoignon, "Influence of the multilayer dielectric mirror design on the laser damage growth in the sub-picosecond regime," *Appl. Opt.* **62**, B126–B132 (2023).
  17. *ISO Standard Nos 21254-1–21254-4* (2011).
  18. S. Hocquet, J. Neauport, and N. Bonod, "The role of electric field polarization of the incident laser beam in the short pulse damage mechanism of pulse compression gratings," *Appl. Phys. Lett.* **99**, 061101 (2011).